

GT2011-46339

**COMBINED EXPERIMENTAL - NUMERICAL APPROACH
FOR THE FUEL JET STUDY IN A LPP COMBUSTOR**

Amedeo Amoresano

Maria Cristina Cameretti

Raffaele Tuccillo

Dipartimento di Meccanica ed Energetica (Di.M.E.), Università di Napoli Federico II
Napoli, Italy

ABSTRACT

The purpose of the paper is the investigation of the phenomena that mainly affect the mixture preparation and the combustion development in lean-premixed chambers supplied with liquid fuels (LPP).

In such a study, the experimental analysis, performed by PDA based measurements, is supported and addressed by a CFD tool that is able to simulate the injection conditions, by isolating and studying some specific phenomena. A 3-D fluid dynamic code (i.e., the FLUENT® flow solver) has been used to simulate the spray pattern in the chamber. Preliminarily, the numerical simulation refer to cold flow conditions, in order to validate the estimation of the fundamental spray parameters through the comparison with the experimental data; in a second step, the calculations employ boundary conditions close to those occurring in the actual combustor operation, in order to predict the fuel vapour distribution throughout the premixing chamber. In particular, the fuel is injected under the typical conditions that occur in the injection system of a gas turbine LPP combustor. In this phase, the experimental information are introduced in terms of air and fuel mass flow rates and of inlet characteristics of the air flow entering the prevaporizing chamber, in order to predict the fuel vapour formation and distribution. The paper also compares different approaches that have been experienced for the CFD simulation.

INTRODUCTION

The liquid fuel used as the energy source must be atomized into smaller droplets in order to increase the surface of fuel exposed to the hot gases and to facilitate rapid gasification and mixing with the oxygen rich ambience. Spray dynamics and combustion studies are extremely important to determine flame stability behavior at widely varying loads, to ensure safety and efficient utilization of energy, as well as to better understanding the mechanisms of pollutants formation and destruction in a gas turbine combustor.

Several authors recently have investigated on this matter in order to guide the development and improvement of modern gas turbine combustion systems, producing significant results both of experimental and numerical type [7- 15]. This paper aims at a contribution in this research field by means of a combined experimental and numerical study for characterizing a swirled spray injected in a LPP gas turbine combustor. The authors start from droplet size and velocity measurements downstream of a Delavan swirling nozzle and, basing on the results from their previous papers [1-4], develop a comparison of several models for simulating the reacting mixture formation in the premixing- vaporizing system.

The experimental activities were performed by means of Phase-Doppler Anemometry (PDA) based measurements [5, 6] for obtaining droplet diameter distributions and velocity data at discrete spatial positions. The 3-D fluid dynamic code (i.e., the FLUENT® flow solver) is used to simulate the spray behaviour in the primary zone of the combustor. The study has required a number of numerical steps to be followed after an experimental validation, and the methodology can be outlined as follows:

- A preliminary simulation has been performed in the first part of the pre-vaporized zone to study the spray in the first phase of the injection when atomization and evaporation occur. In this part, the identification of proper boundary conditions to be assigned for the complete study of the fuel jet atomization both into quiescent environment and under the actual swirled flow conditions; now, the validation of the atomization models (mainly, the well known TAB and Wave models, with the related constants to be assessed) by the comparison with the experimental data.
- The same situations have been studied for hot flow conditions and under the actual pressure, temperature levels and AFR that occur in the gas turbine combustor operation. In this latter case, the analysis of the mixture

formation and of its distribution has been obtained in the whole pre-vaporized zone of the combustor, i.e. in a more complete geometry.

The authors have paid particular attention to the methods for reducing the computational costs of the numerical simulations. In this sense, they have experienced two different approaches. The first one considers the actual flow through the swirled atomizer that is able to provide complete information about the droplet motion conditions at the nozzle outlet. The second is based on a synthetic pressure swirl atomizer model, which is implemented in the commercial flow solver and allows much faster computations. The latter can take advantage of the information provided by the more complete flow model, in terms of a proper assignment of the injection conditions. The comparison of the results from the two approaches is discussed in the final part of this paper.

NOMENCLATURE

- LPP Lean Premixed Prevaporized
- CFD Computational Fluid Dynamics
- PDA Phase Doppler Anemometer
- \dot{m} Mass Flow rate
- AFR Air/fuel ratio

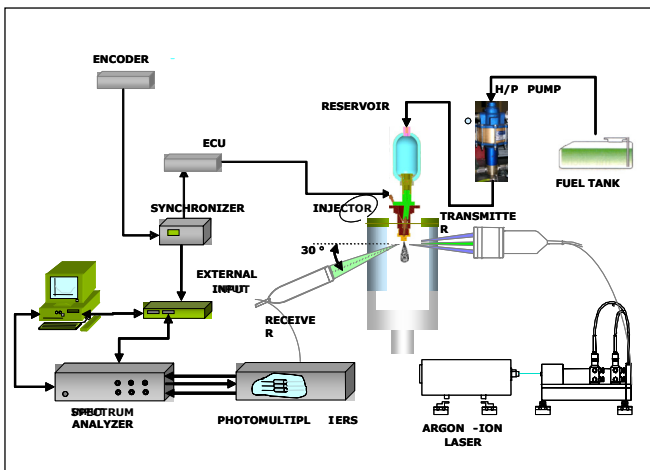


FIGURE 1. Experimental equipment

EXPERIMENTAL RESULTS

The Experimental Setup

The experimental equipment, whose detailed description can be found in papers [1-4], is outlined in figure 1. The spray droplet size and velocity distribution is estimated by using a PDA system [5, 6]. The spray is generated by a commercial pressure swirl atomizer (a Delavan nozzle of the WDA type) with a swirl number of 0.5 and a rated injection pressure of 7 bar (fig. 2). The target half spray angle is of 60°.

The experimental procedure can be summarized as follows: the liquid kerosene, coming from a storage tank, is pressurized with nitrogen contained in a cylinder, and vertically injected into the environment. Finally, kerosene is exhausted into a refuse tank. Droplet sizes and velocities as well as the atomized liquid

concentration have been measured by two-component phase Doppler anemometer. The latter is composed of an Ar- ion laser, as a light source, and a PDA system (Dantec) which includes a Bragg cell, transmitter and receiver probes, and BSA flow to analyze the signals and to acquire the interested output quantities. As said previously, the Bragg cell is used to shift the Doppler frequency; in particular, the frequency imposed is 40 kHz. The focal length is 310 mm. The laser power was typically 25 mW *per beam*. The laser beams wavelength is 514.5 nm and 488 nm for the vertical and horizontal component of the velocity measurement, respectively. Drop sizes assuming spherical particles have been measured in first order refraction. The light scattering angle for kerosene at ambient temperature is 70° that equals Brewster’s angle so that light reflection is completely absent.

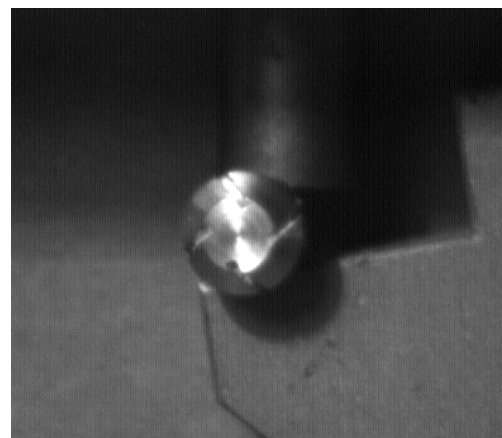


FIGURE 2. Delavan nozzle

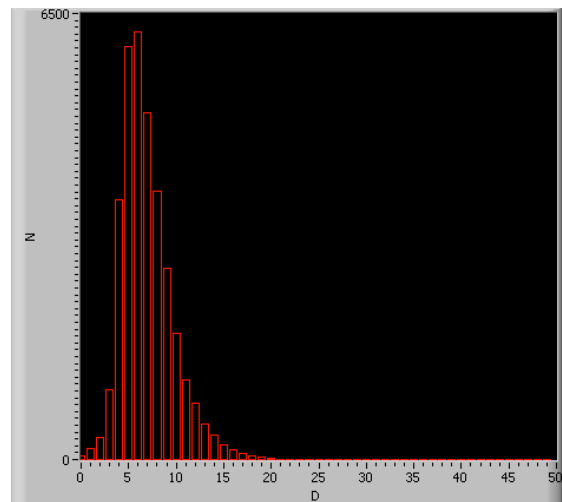


FIGURE 3. Frequency of diameters (at 14 mm from nozzle exit) along the spray axis

Examples of Experimental Data

At each measurement point, the Phase Doppler Anemometer system can give histograms of diameter (fig. 3) and velocity of the droplets within the control volume. From this information, it is possible to derive the mean droplet

diameters and the mean velocities. The PDA measurements of droplet sizes and velocities have been repeated in different planes downstream of the atomizer tip ($x = 0$), from $x = 8$ mm up to $x = 14$ mm (figures 4 and 5). For axial positions lower than 7 mm, the PDA system is not able to validate data due to the high spray density.

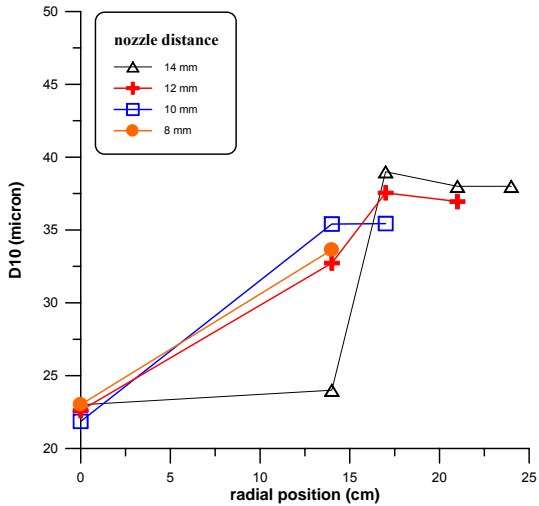


FIGURE 4. Experimental radial profiles D_{10}

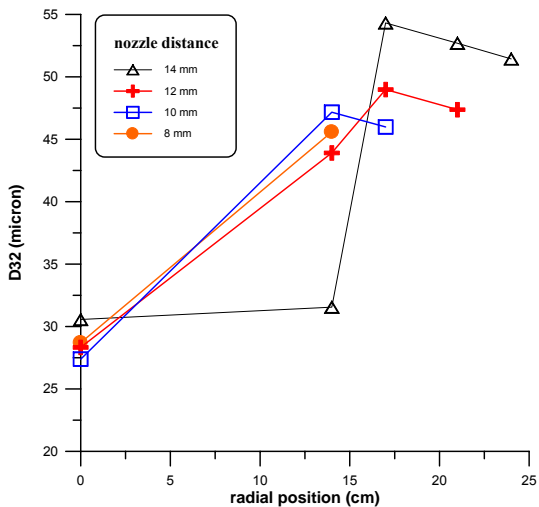


FIGURE 5. Experimental radial values of D_{32} at different distances from nozzle exit

Further droplet size measurements refer to the actual premixing – prevaporizing system, as outlined in fig. 6 that shows a meridional section of the LPP combustor [15] together with a 3-D view of the main and pilot injection systems, as to point out their location within the whole combustor domain of reference. The same figures allow detection of the two radial air inlets with the swirling vanes and of the central position of the fuel nozzle as well.

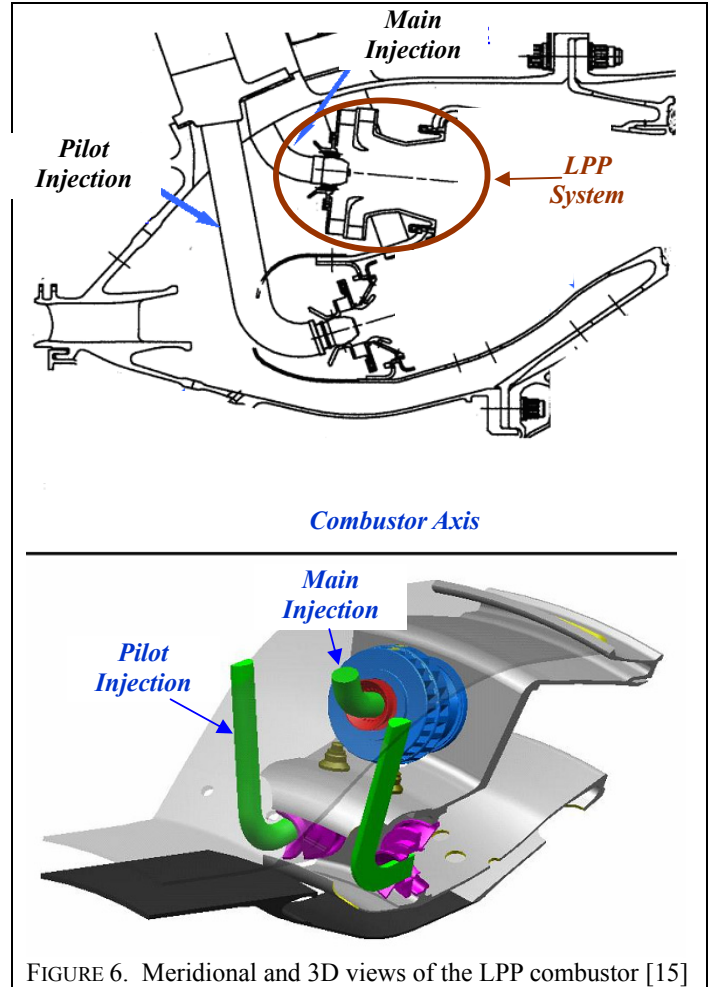


FIGURE 6. Meridional and 3D views of the LPP combustor [15]

Figures 7 and 8 show respectively the D_{10} and D_{32} values along the radial coordinate at the end of the premixing region that is located at 28 mm from the nozzle, i.e. at the exit of the second air swirler of the circled LPP system in figure 6. The curves in these figures compare the distributions of the droplet characteristic diameters that result from different air flow conditions, i.e. with swirled motion at the premixing duct inlet and in quiescent air [10]. The interaction between the swirled air and the fuel reduces the spectrum of diameters (blue line) due to a higher level of the atomization of the droplets. In fact, the mean diameter varies between $7 \mu\text{m}$ and $16 \mu\text{m}$, so that the droplets size distribution inside the duct is more uniform if compared to that in quiescent air. In particular, in figure 7 the mean diameter curve relative to swirled air conditions shows an almost flat behavior except for the points at the periphery where the mean drop size increases because of the interaction with the duct wall. In figure 8, the D_{32} diameters are plotted for both cases. The different formulation of the D_{32} with respect to D_{10} leads to a less evident gap between the droplet diameter distributions that take place with and without the swirled air flow.

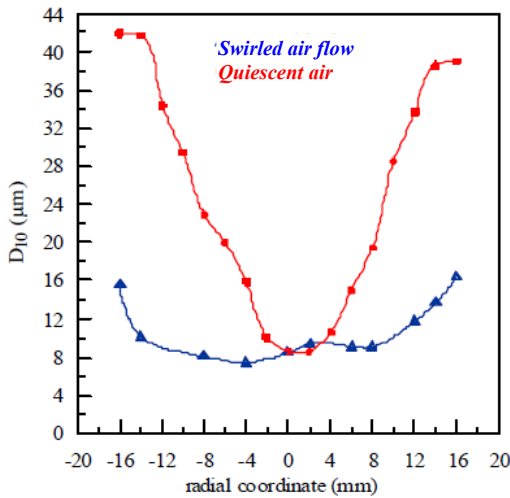


FIGURE 7. D_{10} diameters vs. radial coordinate

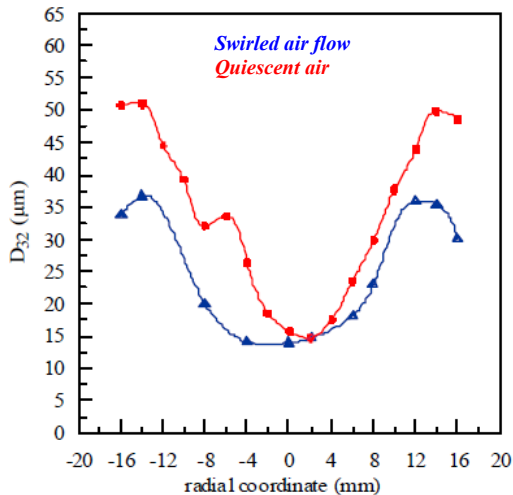


FIGURE 8. D_{32} diameters vs. radial coordinate

COMPUTATIONAL ANALYSIS AND RESULTS

Preliminary Cases

A preliminary investigation of the spray evolution in a first zone of the lean pre-mixing chamber has been performed [4] under cold flow conditions to evaluate only the atomization effect on the spray pattern. For an initial, simplified estimate of the droplet size and velocity, the actual nozzle geometry has not been introduced in the calculations and the spray has been injected into a quiescent ambient by following a typical Lagrangian-Eulerian scheme. The fuel injection system is simulated by a “pressure swirl atomizer” like modeled in the FLUENT® code. Once assigned some typical spray parameters, like cone angle, swirl ratio, injection pressure, initial droplet diameter, the atomizer model returns the droplet size and velocity distribution, so that the interaction with the air

flow is estimated by starting from a given distribution of the droplet discrete flow field.

A more complete, but also more computationally expensive, approach can be followed by considering the actual geometry of the swirling nozzle, like the one outlined in figure 9 and its position within the premixing system of fig. 10. The same figures 9 and 10 also show the nozzle and pre-chamber meshes used in the fully 3D domain. The authors have addressed their preliminary numerical tests to calculate the spray cone angle value, which can be utilized as boundary conditions for the first simulation with the *pressure swirl atomizer*, as described in [3].

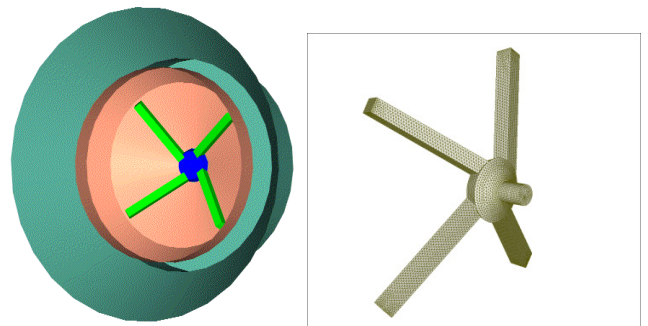


FIGURE 9. Geometrical sketch and computational grid of the internal fuel nozzle

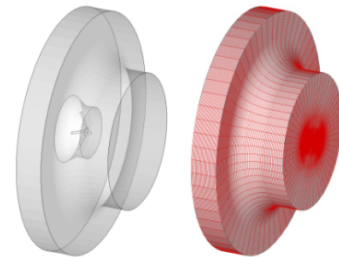


FIGURE 10. First numerical domain of pre-mixing chamber

Table 1. Fuel and Injection characteristics

Fuel	<i>kerosene</i>	
Fuel density	900	kg/m ³
Fuel viscosity	3.0 10 ⁻⁶	m ² /s
Mass flow rate	3.15 x 10 ⁻³	kg/s
Pressure	7	bar
Temperature	288	K

In the table 1, the injection characteristics that have been assumed in the numerical simulations are reported. In order to predict the break-up phenomenon, the authors have used two different atomization models (i.e., the TAB and WAVE models [16-18]) implemented in the Fluent® solver and the results are compared in terms of droplet diameters. As reported in previous works [3-4], the Wave model leads to results more similar to

the experimental ones, while the TAB model underestimates the droplet diameters. In the figures 11 the mean diameter values (D_{10}) are plotted to confirm this assertion and they are compared with the experimental data. In figure 12, the D_{32} values are reported at different distances from nozzle exit. The diagram confirms the progress in the spray cone spreading if proceeding along the axial direction, but only a qualitative agreement can be detected with the experimental distributions in figure 5. Such results, together with those presented in the next section, suggest that a further numerical effort is needed for a proper calibration of the atomization models.

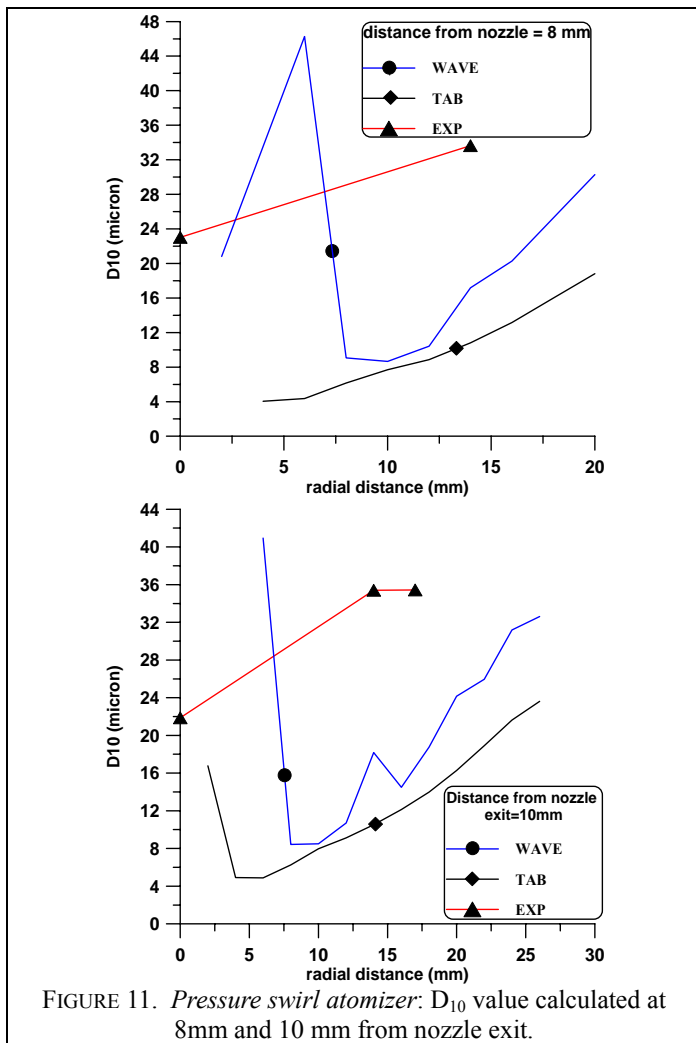


FIGURE 11. Pressure swirl atomizer: D_{10} value calculated at 8mm and 10 mm from nozzle exit.

In the following calculations a more complex geometry was considered (fig. 10), due to the nozzle presence which permits to simulate the actual swirl motion of the fuel injected in this case in quiescent ambient (with a block-structured mesh of 435000 cells). The spray distribution indicates smaller droplet diameters when the TAB model is used (fig. 13): these results are consistent both with those from technical literature and with the experimental – numerical matching in fig. 11. A comparison between the diameters obtained with quiescent and swirled air

(fig.14) has been plotted in fig. 15 and 16 by using the WAVE model. The swirled air aids a faster break-up of the droplets especially in the external boundary as demonstrated also in the experimental results reported in figure 6.

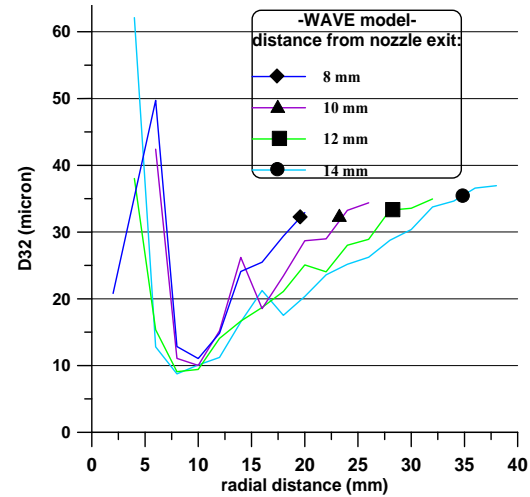


FIGURE 12. Pressure swirl atomizer: D_{32} value calculated at different distances from nozzle exit.

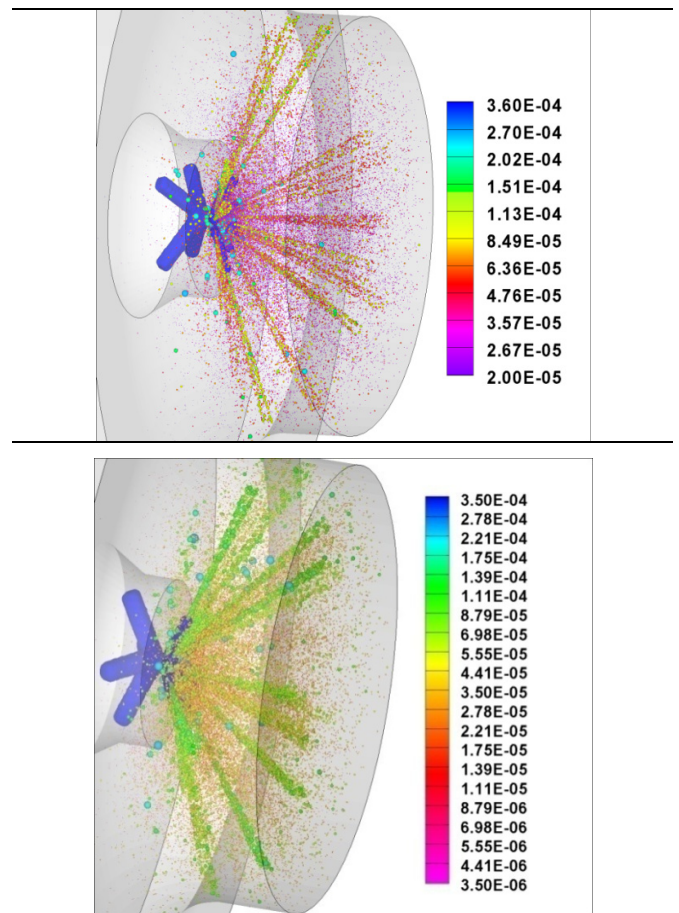


FIGURE 13. Droplets diameter distribution in a pre-mixing chamber. Wave model and TAB model. Quiescent ambient.

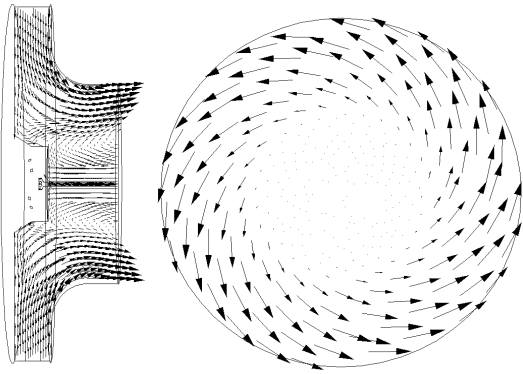


FIGURE 14. Air velocity field in the pre-chamber

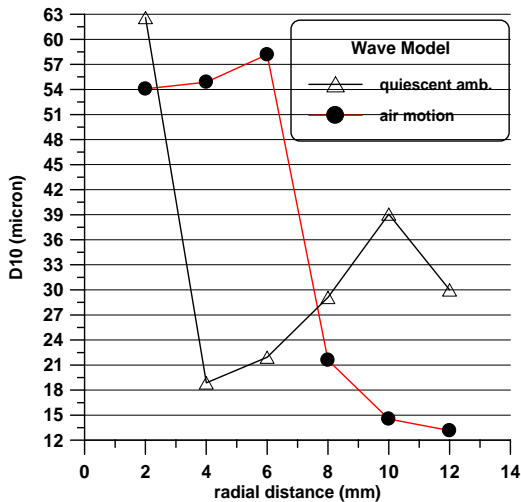


FIGURE 15. D_{10} values calculated at 8 mm from nozzle exit. Quiescent ambient and air swirl motion

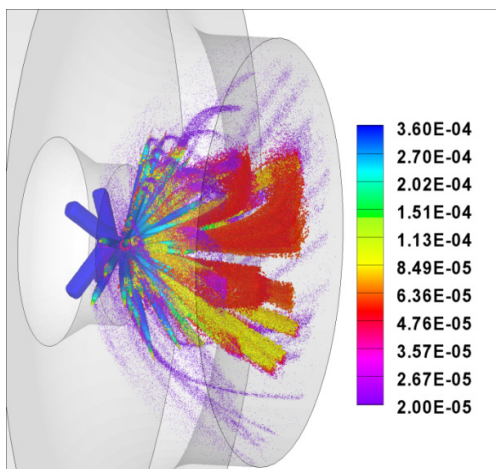


FIGURE 16. Wave model. Droplets diameter distribution in a pre-mixing chamber with swirled cold air motion.

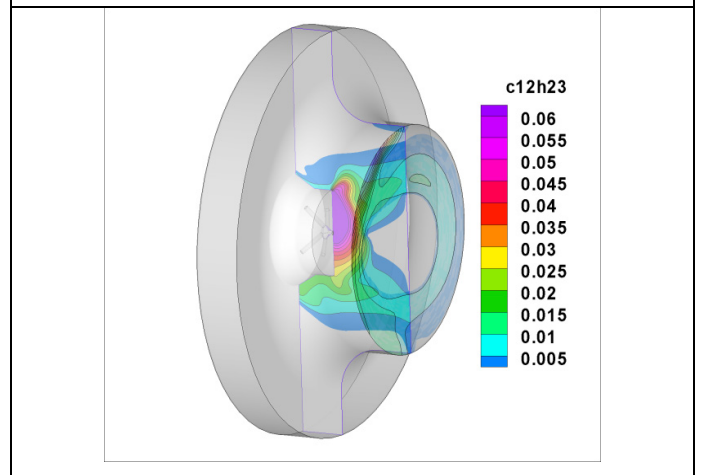
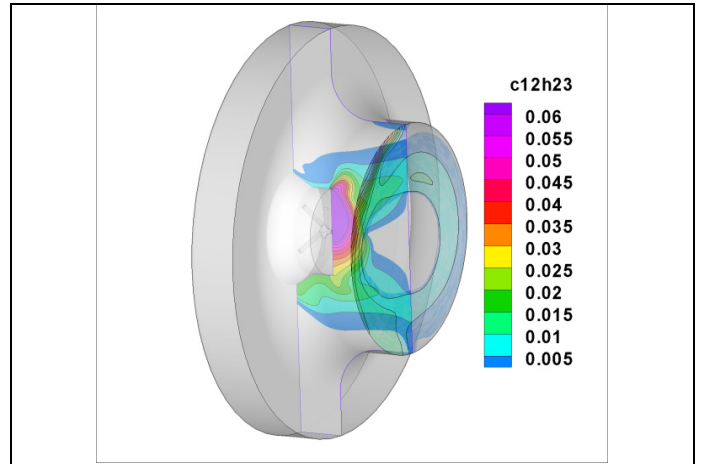


FIGURE 17. Fuel vapour distributions for swirled motion (hot flow). TAB and Wave models.

Table 2. Evaporating conditions	
Fuel	kerosene
AFR	25
Air swirl angle	variable
Air Mass flow rate	0.0787 kg/s
Pressure air	18 bar
Temperature air	800 K

The same situations have been studied not only for cold flow conditions but also under the actual pressure and temperature levels that occur in the gas turbine combustor to evaluate the evaporation effect. In the latter case, the study is completed by the analysis of the mixture formation and of its distribution at the premixing outlet. In table 2, the operating conditions are reported. As an example of the previous calculations performed in the reduced geometry of the pre-

evaporating zone [4], the fuel vapour distributions is reported in fig. 17: the fuel-air mixing, estimated with the actual levels of inlet air velocity, starts with an evident asymmetry that can be related to the spatial location of the four liquid channels. However, an almost regular behaviour in the peripheral direction is reached by the mixed jet at increasing distances from the injector. The same figure suggests that the more feasible choice is the Wave atomization model, as already indicated by the previous comparisons with the available experimental data. Actually, the TAB model would estimates a too fast droplet atomization (fig. 13) and therefore an early fuel evaporation, so in contrast with the purpose of the LPP system.

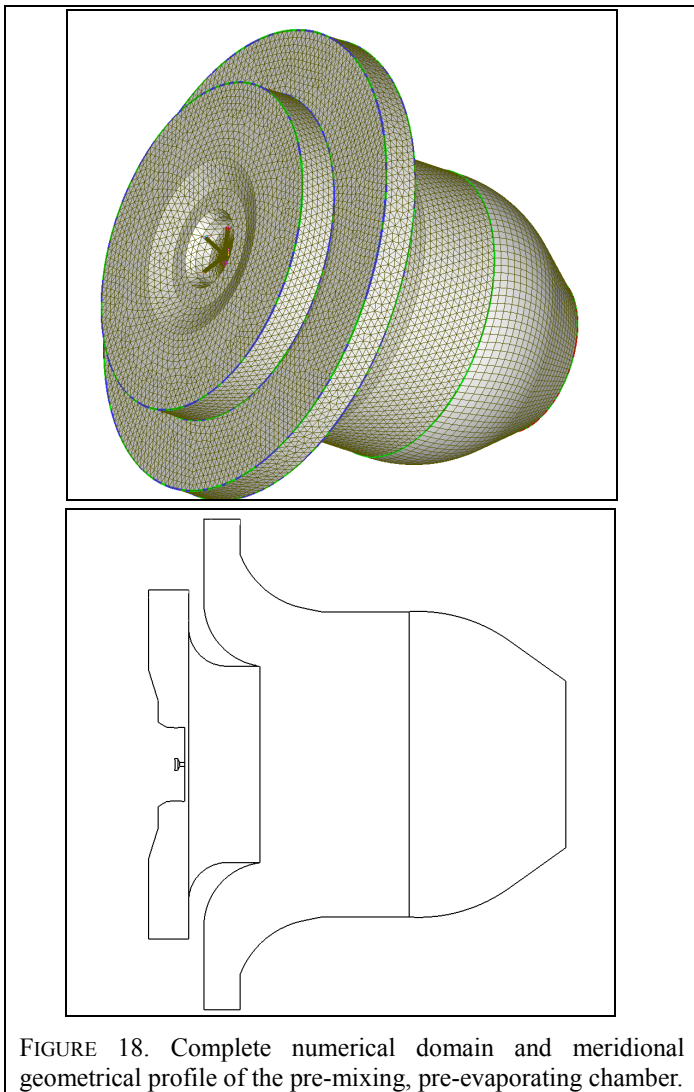


FIGURE 18. Complete numerical domain and meridional geometrical profile of the pre-mixing, pre-evaporating chamber.

Evaporating cases with the complete LPP geometry

A new mesh referring to the complete geometry of the pre-mixing, pre-evaporating device, whose location is evidenced in fig. 8, has been used for the next simulation under evaporating conditions (fig. 18). After a grid dependence analysis, the mesh size convergence was established with 400000 cells of the mixed hexahedral – tetrahedral type. Actually, the resulting

average size and, mainly, the average distance between two neighboring vertices, of 2.2×10^{-4} m, ensure a satisfactory resolution of the droplet trajectories. Details of the meshed injector are detectable in fig. 9. The related computational cases have been performed under the same injection conditions as for the previous cases (table1) with the *Pressure swirl atomizer*. The computational cases discussed in this section, like those previously described, were carried out by solving the turbulent flow throughout the domain with the standard *k-ε* model and the continuous - discrete phase interaction with the Lagrangian – Eulerian approach implemented in the FLUENT® code.

Basing on the preliminary estimations of the droplet distributions shown in figure 13, which result from the calculations in the computational domain in fig. 10, some key parameters like the initial half cone spray angle and the dispersion angle were set properly: values of 60° and 6° , respectively, were assigned and these data are in accordance with both the experiments and the rated values for the Delavan injector. Other parameters, like the liquid sheet constant and the ligament constant, were left at the default values of 12 and 0.5, respectively.

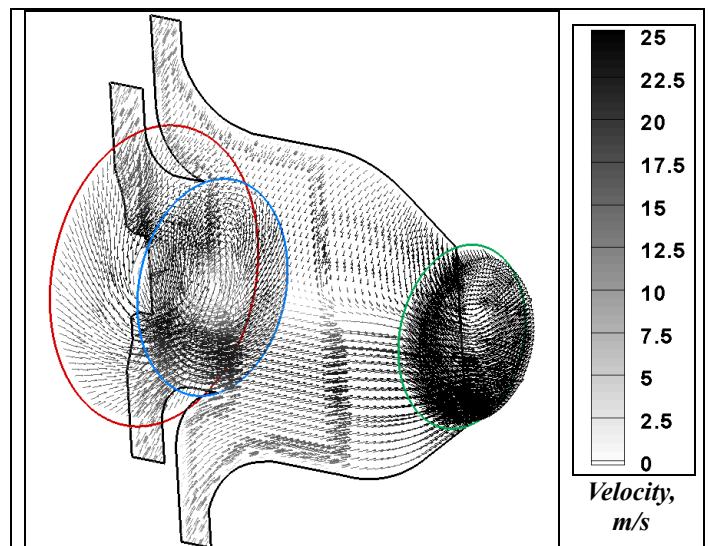


FIGURE 19. Air velocity vectors field. Swirl 45° .

A sensitivity analysis to the air swirl motion intensity was obtained by assuming variable inclinations of the swirling blades in the two circumferential air inlets (actually, the domain geometry does not include the blades). In particular, three cases were considered: with 45° , 25° and 50° of slope of the swirled inlet air flow with respect to the radial direction. A typical velocity vector field is represented in figure 19, with reference to the air flow that results in the first computational case.

A comparison between the results in terms of fuel mass fraction and velocity vectors allows us to detect the best mixing condition. In the figures 20, 21 and 22 the fuel mass fraction contours are reported in two different planes. The asymmetries that can be detected in the fuel vapour distributions can be explained by the non-uniform value of the initial droplet diameter, which follows a probabilistic Rosin – Rammler function.

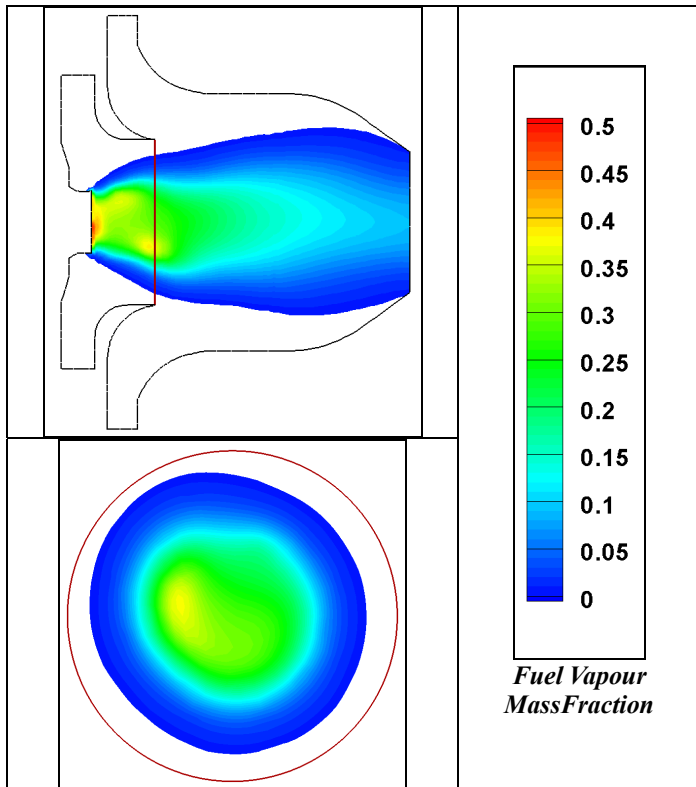


FIGURE 20. Fuel mass fractions distribution in a meridional plane and in an internal plane. Swirl 45° .

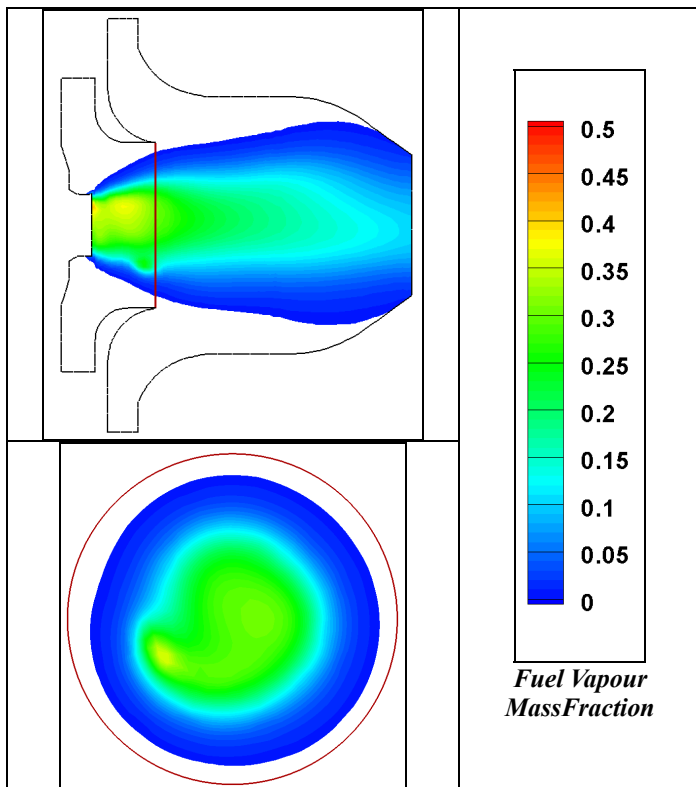


FIGURE 21. Fuel mass fractions distribution in a meridional plane and in an internal plane. Swirl 50° .

The vapour distribution asymmetries extinguish when proceeding towards the prevaporizer exit and they are more relevant for lower values of the air swirl angle (fig. 22). Actually, the variable inlet conditions and the resulting air motion influence the droplets distribution, atomization and the consequent evaporation as shown also in the figure 23 where the three different swirl angles have been considered. In the second case (i.e., 25°), the spray cone angle is relevantly reduced while an increased jet opening can be observed for the higher values of the swirl angle. As a consequence, both in the meridional plane and in cross sections of the pre-mixing chamber the fuel vapour is more concentrated within the central area (fig. 21), while in the third case (50°) the vapor presents a wider, more uniform, distribution in the same plane (fig. 22) also with respect to the baseline case in fig. 20 with a swirl angle of 45° .

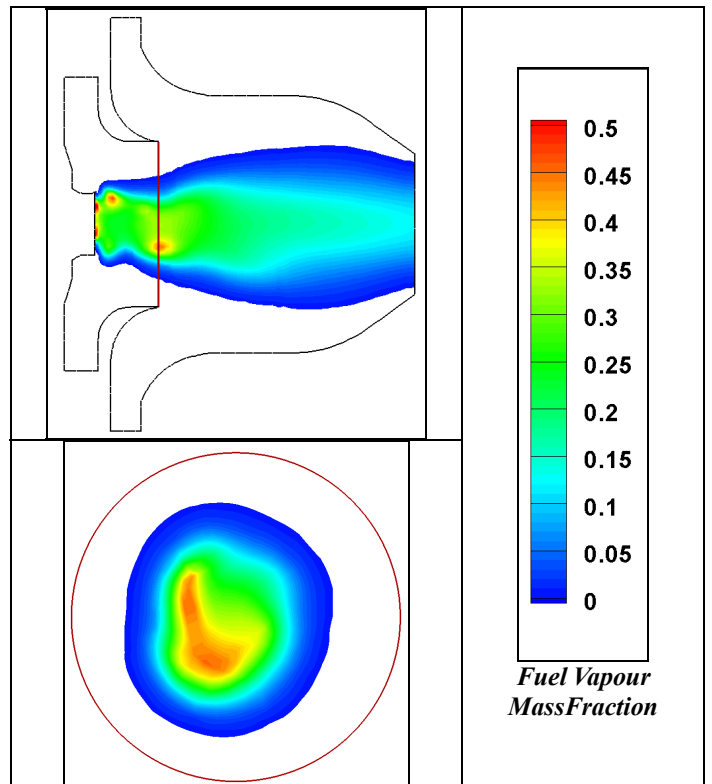


FIGURE 22. Fuel mass fractions distribution in a meridional plane and in an internal plane. Swirl 25° .

In figure 24, the fuel mass fraction distribution in the outlet surface with the three swirl values is represented as to highlight the differences among the three swirled air conditions. In all cases, the asymmetries disappear but in the third one (50° swirl) the contours confirm the previous considerations about the better uniformity of the fuel concentration. In figure 25 the fuel mass fraction versus the radial coordinate in the outflow plane of the pre-mixing, prevaporizing zone is plotted for every case considered. As expected, the case with 50° presents the best distribution also along the radial direction. It should be observed that the curves in fig. 25 are obtained by a polynomial fitting of the actual values, whose scattering is however very

limited even in the most challenging condition that is induced by the air swirl angle of 25° (fig. 26).

It should be underlined that the predicted spray pattern and air-fuel mixing are strongly affected by the value assigned to the ligament constant. Therefore, future numerical activities should include a sensitivity analysis to such a constant.

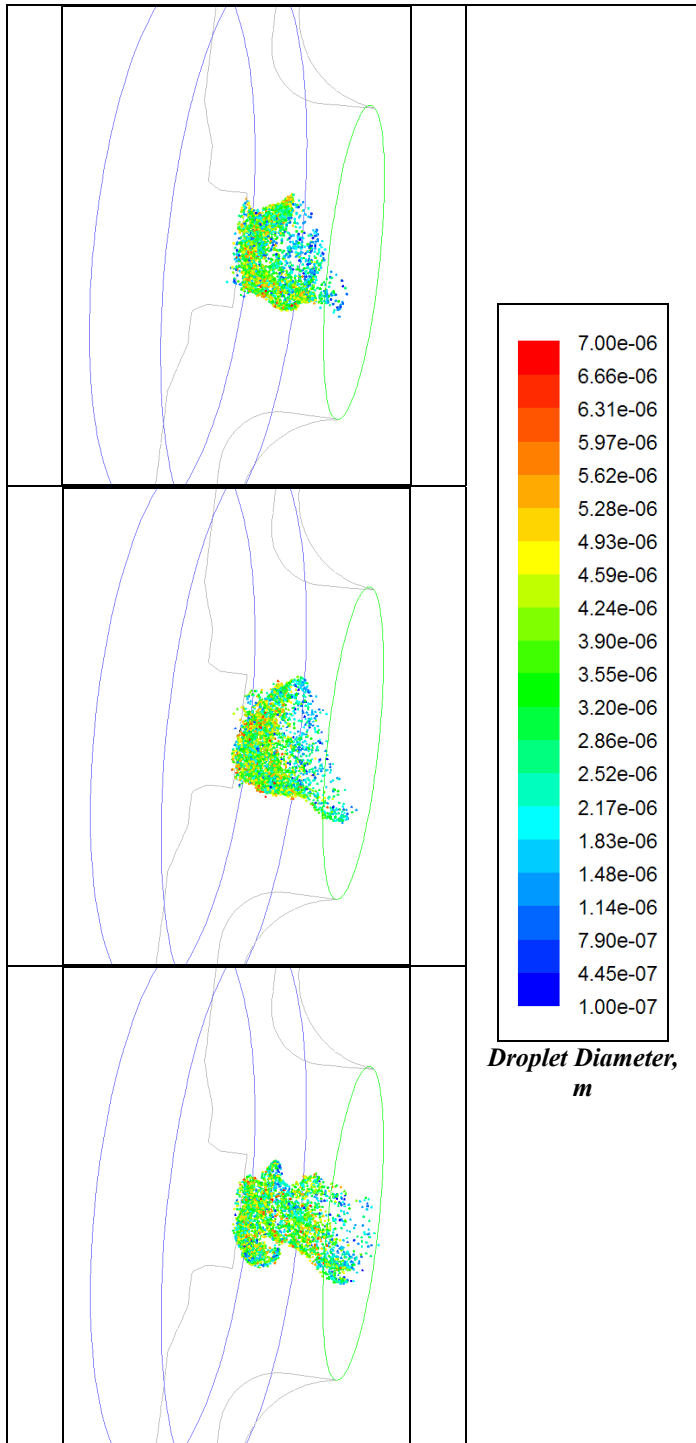


FIGURE 23. Droplet diameter distribution in the pre-chamber with three swirl values: 45°, 50° and 25° respectively.

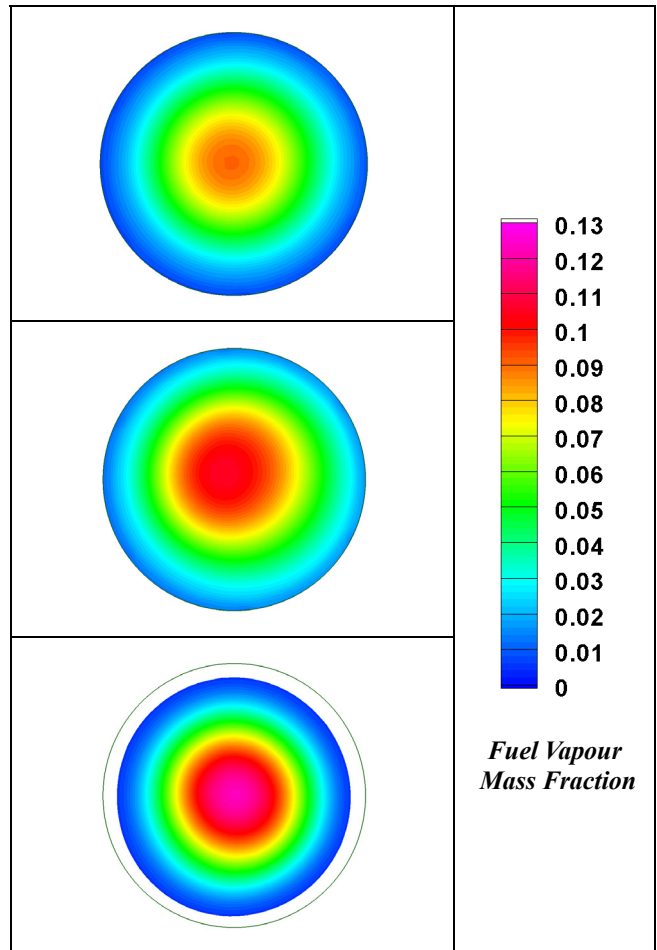


FIGURE 24. Fuel mass fraction distribution in the outlet surface with three swirl values: 45°, 50° and 25° respectively.

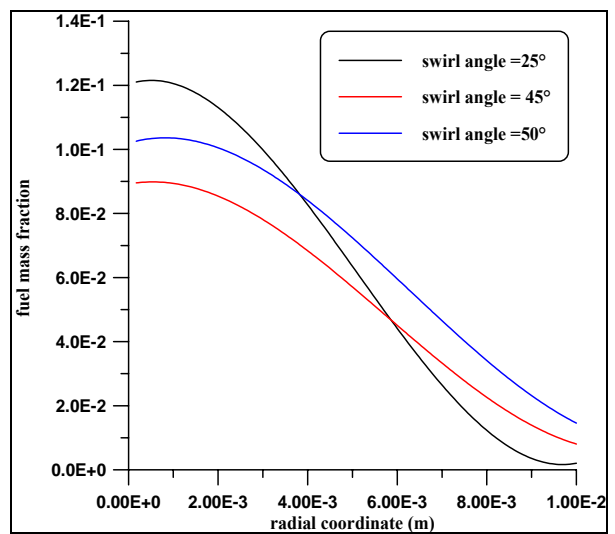


FIGURE 25. Fuel mass fraction versus radial position in the outlet surface with three swirl values.

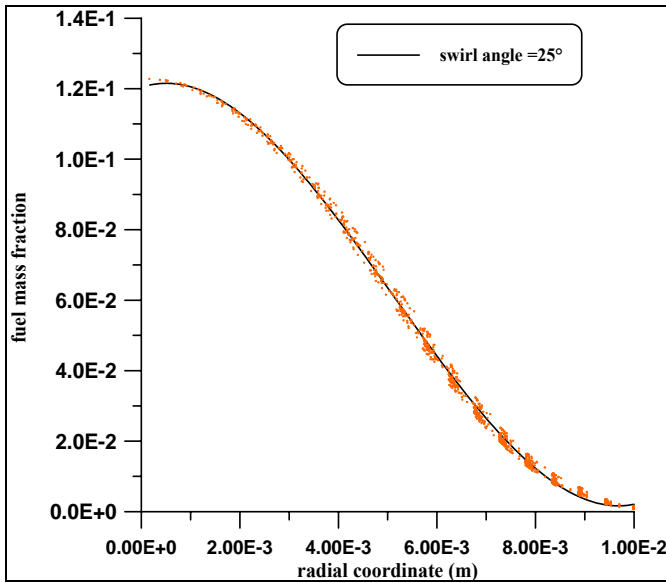


FIGURE 26. Fuel mass fraction versus radial coordinates.

The droplet flow simulation in the atomizer channels

The last results discussed above refer to the adoption of a typical model that is already implemented in the flow solver for taking into account the effects of a pressure swirl atomizer. An alternate method has been experienced by the authors, basing on the full simulation of the liquid droplet flow throughout the ducts of the injector (fig. 9). This approach allows the computations to proceed with no further assignments but the liquid inlet velocity and flow rate. In this way the spray angle, together with the droplet size distribution at the atomizer outlet, are returned from the calculations and the swirled droplet motion itself is automatically predicted. After a sensitivity analysis on the effects of the initial liquid velocity, an example of the application of this method is given in the following, with reference to the standard fuel flow rate (table 1) and a liquid velocity of 20 m/s at the inlet of the channels. The inlet air swirl angle was set at 45° , basing on the results in figures 20 – 24, as previously discussed. Basing on the considerations in the above sections, the atomization Wave model was adopted, together with the standard evaporation model as implemented in the FLUENT® code.

Figure 27 displays the particle displacement in a meridional plane and the axial distribution of droplet diameters. The first diagram allows estimation of the initial opening angle of the hollow cone and of its thickness, with a good agreement with the rated injector data. The second one shows the progress in the droplet expiration along axial flow paths. Compared with the experimental data in fig. 6, that refer to cold flow conditions, a reasonable situation can be detected in this figure since the combined effect of the droplet breakup and of a relevant evaporation rate leads to a faster extinguishment of the atomized jet. Actually, at the same distance of 28 mm from the atomizer exit as for the data in fig. 6, the average diameter has dropped down to $1 \mu\text{m}$.

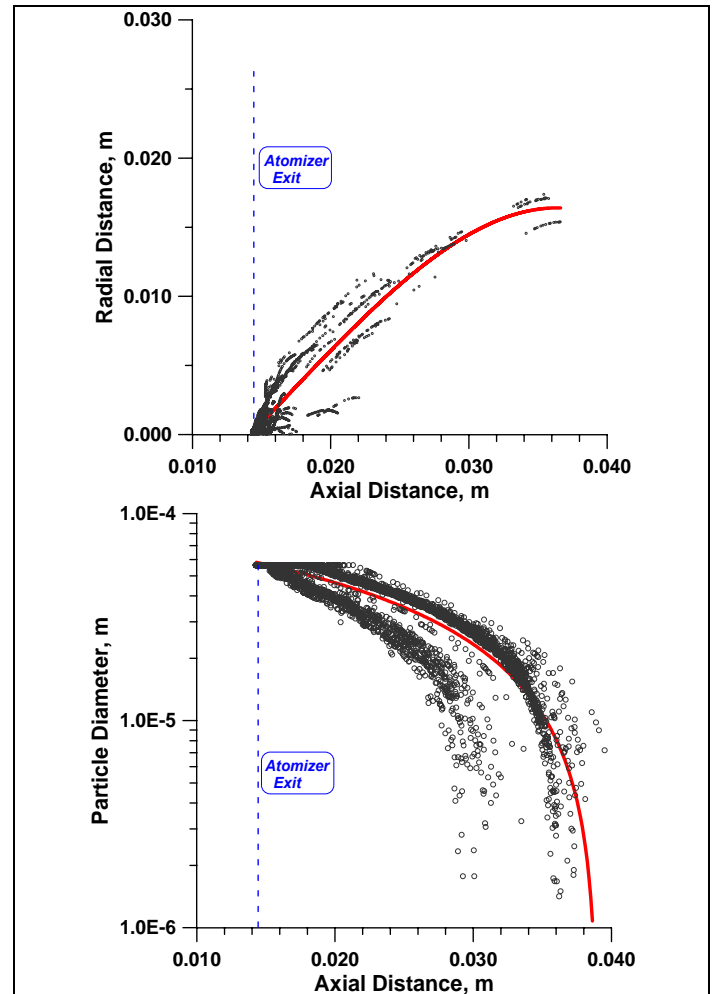


FIGURE 27. Droplet displacement and diameter distribution in the liquid fuel jet

The droplet spatial distributions in fig. 28 put into evidence the computed jet pattern and the trajectories that result from the effect of both the swirling atomizer and the air vorticity. In order to emphasize the typical helical path of the droplets, this figure and the following one were drawn with a 1:10 skip ratio. The droplet penetration in the LPP system can be also detected. As a further proof of the interaction between the continuous and the discrete phase, the following figure 29 displays the droplet velocity vectors superimposed to the air flow field in a cross section at 15 mm from the atomizer exit.

Finally, figure 30 shows the development of the fuel vapour distribution throughout the premixing – prevaporizing system. The mass fraction contours exhibit a progressive regularity if proceeding towards the LPP outflow. At the latter station, a nearly axisymmetric distribution is achieved with the maximum concentrations within the central zone. This represents a satisfactory condition for a correct ignition of the reacting mixture in the neighboring primary region of the combustor.

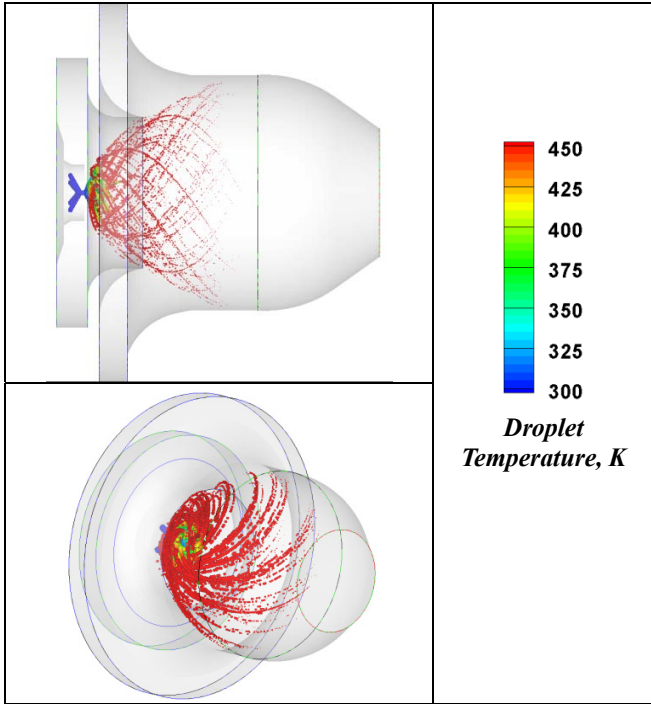


FIGURE 28. Spatial distributions of the atomized swirled jet.

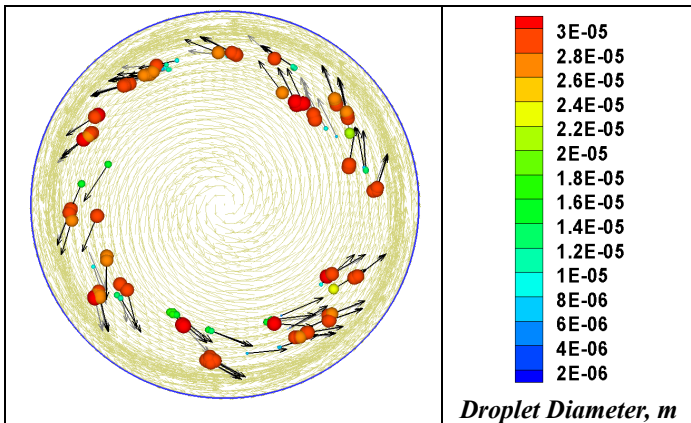


FIGURE 29. Droplet and air velocity vectors in a cross section.

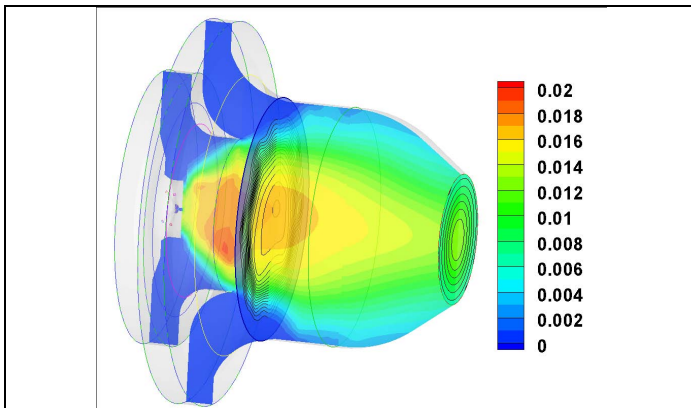


FIGURE 30. Fuel vapour mass fraction in the LPP domain

Finally, it is of interest to observe that the fuel vapour contours in fig. 30 are in fair agreement with those displayed in the previous figures 20 – 22, which were obtained with the pressure swirl atomizer model. Nevertheless, it can be observed that the liquid evaporation is delayed with respect to the one resulting from the adoption of the synthetic model. This is due to the higher value of the average droplet diameter at the nozzle exit, so that indications may be derived for a more proper assignment of the initial conditions for the synthetic model.

The last consideration suggests that the proposed methodology, whose disadvantage is represented by the relevant computational cost, may be employed for a preliminary calibration of more affordable models of the fuel atomizer, in order to set up and perform faster numerical simulation with more correct assumptions for the atomizer inlet data.

CONCLUSIONS

This study has been carried out through the experiments and the numerical simulations of a spray under atomization and evaporation conditions in the premixing duct of a gas turbine LPP combustor. The experimental measurements have been obtained by the PDA method for estimating the droplet size.

The Fluent® flow solver has been used in the CFD based analysis of the spray. The characterization of both the fuel droplet distribution and its mixing with air plays a key role for the choice of the atomization technology and its optimization in terms of homogeneity of the fuel/air mixture. The authors addressed this task by comparing two different approaches of increasing complexity and computational costs. Of particular interest appears to be the possibility of a direct simulation of the liquid droplet motion inside the atomizer. This leads to a complete characterization of both the spray cone pattern and the droplet velocity distribution at the nozzle exit. The related results may be employed for setting up proper calculations based on synthetic models of the atomizer, so involving more reasonable computational times. In this case, further analyses should be specifically addressed to the calibration of some constants that strongly affect the spray pattern and the droplet atomization development. In this sense, the results discussed in this paper must be intended as a first attempt to appreciating the potential of different methods for the LPP system simulation. Once a satisfactory model refinement will be reached, both the approaches will allow a more comprehensive estimation of the correct operation of the premixing – prevaporizing system.

The calculated results encourage going deep into the study of the base phenomena that mainly affect the combustion development in a low-emission, stationary combustion chamber for gas turbine application. The future analyses will therefore deal more directly with the combustion development in the primary zone of the combustor and the authors will therefore focus their attention on more complex geometries.

ACKNOWLEDGMENTS

The CFD calculations are licensed by *Fluent Inc.*

REFERENCES

- [1] Amoresano, A., Cameretti, M.C., Tuccillo, R., 2007, "Investigation by High Speed Imaging of Instability on the Boundary Lines of an Hollow Cone Spray", Combustion Meeting, Creta, april 2007, art.15/13.
- [2] Amoresano, A., Cameretti, M.C., Tuccillo, R., 2007, "Experimental and Numerical analysis of Instability on the Boundary Lines of an Hollow Cone Spray", proc. of 23rd ILASS Europe Conference.
- [3] Amoresano, A., Cameretti, M.C., Tuccillo, R., 2010, "Experimental and Numerical Characterization of the Fuel Jet in LPP Combustor", proc. of ASME-ATI-UIT 2010 Conference on Thermal and Environmental Issues in Energy Systems.
- [4] Amoresano, A., Cameretti, M.C., Tuccillo, R., 2010, "CFD and Experimental Study in a LPP Chamber", proceedings of 65° Congresso Nazionale ATI, Cagliari, sept. 2010.
- [5] Tropea C. and Damaschke N., New developments in phase doppler anemometry, Journal of Visualization Volume 2, Numbers 3-4 / September, 2000 pp 273-279
- [6] Jin Seok Kim and Jeong Soo Kim , A characterization of the spray evolution by dual-mode phase doppler anemometry in an injector of liquid-propellant thruster, Journal of Mechanical Science and Technology Volume 23, Number 6 / June, 2009 pp. 1637-1649.
- [7] Dikshit, S., Channiwala, S., (2009), Experimental Investigations of Performance Parameters of Pressure Swirl Atomizer for Kerosene type Fuel, ASME paper GT-2009-59082
- [8] Kashdan, J.T., Shrimpton, J.S., Characteristics of transient, swirl-generated, hollow-cone sprays, Atomization and sprays; Vol.16; pp. 493-510; 2006.
- [9] Meier, U., Heinze, J., Hassa, C., Response of spray and heat release to forced air flow fluctuations in a gas turbine combustor at elevated pressure, ASME paper GT2007-27310.
- [10] Hage, M., Dreizler, A., Janicka, J., Flow fields and droplet diameter distributions of water and n-heptane sprays at varied boundary conditions in a generic gas turbine combustor, ASME paper GT2007-27108.
- [11] Marchione T., Allouis C., Amoresano A., Beretta F., Preliminary Study of Hollow-Cone Spray by PDA Analyzer for LPP Conduct, Joint Meeting of the Greek and Italian Sections of Combustion Institute.
- [12] Cameretti M.C., Tuccillo R. (2005), A CFD Based Off-Design Study Of Micro-Gas Turbines Combustors, ASME paper GT-2005-68924.
- [13] Hage, M., Brübach, J., Dreizler, A., 2010, Velocity and droplet distributions of reacting N-heptane sprays at varied boundary conditions in a generic gas turbine combustor, ASME paper 2010-23378
- [14] Levy, Y., Gany, A., Goldman, Y., Erenburg, V., Sherbaum, V., Ovcharenko, V., Rosentsvit, L., Chudnovsky, B., Herszage, A., Talanker, A., Increasing Operational Stability in Low Nox GT Combustor by a Pilot Flame, ASME paper 2010- 22785
- [15] Colantuoni, S., Di Martino, P., Cinque, G., Terlizzi, A., The Development of Low NO_x CLEAN Combustor in the Frame of the EEFAE Research Program, ASME paper GT2010-27857
- [16] O'Rourke P.J., Amsden, 1987, A.A, The TAB Method for Numerical Calculation of Spray Droplet Break up, SAE paper 872089.
- [17] Reitz R.D., Diwakar R., 1987, Structure of High-Pressure Fuel Sprays, SAE paper 870598.
- [18] Reitz R.D., 1987, Modelling Atomisation Processes in High-Pressure Vaporising Sprays, Atomisation and Sprays Tech., vol.3, pp. 309-337.